



Reversible charge storage in a single silicon atom

Amandine Bellec,^{1,2} Laurent Chaput,^{3,4} Gérald Dujardin,¹ Damien Riedel,^{1,*} Louise Stauffer,³ and Philippe Sonnet³

¹*Institut des Sciences Moléculaires d'Orsay, ISMO, UMR 8214, CNRS, Université Paris Sud, 91405 Orsay Cedex, France*

²*Laboratoire Matériaux et Phénomènes Quantiques, Université Paris Diderot Paris 7, Sorbonne Paris Cité, CNRS, UMR 7162, case courrier 7021, 75205 Paris cedex 13, France*

³*Institut de Science des Matériaux de Mulhouse, IS2M, UMR 7361, CNRS, Université de Haute-Alsace, 3b rue A. Werner, 68093 Mulhouse, France*

⁴*Institut Jean Lamour, UMR CNRS 7198, Nancy Université, Bd. des Aiguillettes, BP 23, 54506 Vandoeuvre Les Nancy Cedex, France*

(Received 12 September 2013; published 10 December 2013)

The ultimate miniaturization of electronic devices at the atomic scale with single electrons requires controlling the reversible charge storage in a single atom. However, reversible charge storage is difficult to control as usually only one charge state can be stabilized. Here, combining scanning tunneling microscopy (STM) and density functional theory (DFT), we demonstrate that a single silicon dangling bond of a hydrogenated *p*-type doped Si(100) surface has two stable charge states (neutral and negatively charged) at low temperature (5 K). Reversible charge storage is achieved using a gate electric field between the STM tip and the surface.

DOI: [10.1103/PhysRevB.88.241406](https://doi.org/10.1103/PhysRevB.88.241406)

PACS number(s): 68.35.bg, 07.79.Cz, 31.15.E-, 52.80.Wq

Single-atom electronics is of both fundamental and technological interest. A number of elementary effects, including single-atom transistor^{1,2} and single-atom Kondo effect,³ have been recently demonstrated.^{4–7} To achieve not only single-atom but, moreover, single-electron operation, it is crucial to control the charge state of a single atom. Single-electron charging has been performed with single atoms^{8,9} and molecules^{10,11} weakly interacting at low temperature with an insulating layer^{8–10} or a metallic substrate through van der Waals interactions.¹¹ Semiconductor silicon surfaces passivated by hydrogen^{12–15} or boron^{16,17} atoms offer unique opportunities to manipulate the charge states of single atoms strongly interacting, via chemical bonds, with the substrate. Indeed, on passivated silicon surfaces, the removal of a single hydrogen or boron atom creates a silicon (Si) dangling bond (DB) state whose energy lies within the substrate band gap where no delocalized surface state exists. As a consequence, the Si dangling bond state is well localized and only weakly coupled to other electronic surface states. Recently, it has been shown that, for the *n*-type doped hydrogenated Si(100) surface, Si dangling bonds are negatively charged and their charge state is modified by Coulomb interaction with neighbor Si dangling bonds.^{12–15} However, their charge state is fixed and cannot be varied at will, unless one modifies the positions of the dangling bonds relative to each other, which is hardly feasible. On boron passivated Si(111) surfaces, the Si dangling bond is positively charged and one can access its neutral and negative charge states only when a high tunnel current passes through the dangling bond.^{16,17} In this case, the neutral and negative charge states are not stable, even at low temperature, and the Si dangling bond recovers its initial positive charge state as soon as the tunnel current is switched off.

In this Rapid Communication, we show that, on a *p*-type doped hydrogenated Si(100) surface, Si dangling bonds (Si-DB) have two stable charge states (neutral and negative). The reversible charging and discharging of a single Si-DB, i.e., the reversible transition between the two stable charge states, is activated by using a gate electric field between the tip of a STM located on top of the dangling bond and the surface.

These results are explained by spin-polarized DFT calculations of the Si dangling bond state energy.

The experiments are performed on hydrogenated surfaces of degenerate *n*-type (As, $\rho = 5 \text{ m}\Omega \text{ cm}$) and *p*-type (B, $\rho = 5 \text{ m}\Omega \text{ cm}$) doped Si(100). Varying the type of doping is crucial as it enables to move the Fermi level of the substrate relative to the charge states of the Si dangling bonds and thus to explore the best conditions for charging and discharging the Si dangling bonds. The hydrogenation of the surface is performed in situ in ultra-high vacuum (UHV) as previously reported.²³ A low temperature (5 K), UHV STM is used to image and manipulate the Si dangling bonds.

Calculations are performed using a 6×6 slab containing four silicon layers. The silicon bottom layer is saturated with hydrogen atoms as well as the silicon top layer except for one Si atom, which simulates the individual Si-DB. Thus the total number of atoms in the slab is 251. To take into account the effect of the dopant type, one silicon atom is replaced by one arsenic (As) or one gallium (Ga) dopant atom for *n*- and *p*-type doped silicon calculations, respectively. Here, a Ga dopant atom is chosen instead of a B (boron) dopant atom in order to minimize the deformation of the silicon surface, which would occur with a boron atom. Indeed, the strong surface deformation calculated with boron is artificial as, in reality, the dopant atom might be deeper than in the slab used here. The whole system, apart from the H bottom layer, is allowed to relax until the forces on each ion are lower than $0.01 \text{ eV}/\text{\AA}$. The spin polarized electronic structure has been calculated with 10 *k* points using the LAPW method as implemented in the WIEN2K code.¹⁸ The exchange and correlation effects are treated by the Perdew-Burke-Ernzerhof generalized gradient approximation functional.¹⁹ The calculated gap energy is equal to 1.14 eV. Note that the number of silicon layers and *k* points considered in our simulations (i.e., four layers and 10 *k* points) is sufficient to provide converged electronic states for both *n*- and *p*-type doped silicon samples. This results in a calculated surface gap energy that is similar to the one obtained in previous work.^{20–22}

The numerical simulation of the tip-induced band bending is performed by solving the 2D Poisson equation upon the STM junction.²⁹ The calculation code uses a tungsten tip with a radius of curvature of $R = 50$ nm separated from the surface by a distance $d = 1.0$ nm. The band gap of the silicon surface is set at 1.1 eV with a donor concentration of $4.7 \times 10^{19} \text{ cm}^{-3}$. For these simulations, the conduction band and valence band effective mass of the carrier is taken equal to $0.34m_e$ and the silicon dielectric constant is 11.9 at 5 K.

The STM topographies of a single Si-DB are compared in Fig. 1 for hydrogenated p -type and n -type doped Si(100) surfaces in the occupied ($V_S < 0$) and unoccupied ($V_S > 0$) states.^{23,24} A single Si-DB results from a missing hydrogen atom of a dihydride dimer.²⁴ Such Si-DBs are residual dangling bonds remaining after the hydrogenation process. To verify that these bright features are indeed Si dangling bonds, the hopping of the neighbor hydrogen atom to the Si-DB site is activated with the STM tip as described in Refs. 21–25. For p -type doping, the Si-DB appears bright both in the occupied and the unoccupied state topographies [see Figs. 1(a)–1(c)]. For n -type doping, the Si-DB appears bright in the occupied state STM topography while it appears surrounded by a dark halo in the unoccupied state [see Figs. 1(d)–1(f)]. The dark halo, also observed at room temperature,^{12,25} has been assigned to a charge screening effect due to the negative charge of the Si-DB.^{12,25,26} On the contrary, for p -type doping, the STM topographies [see Figs. 1(a) and 1(b)] do not show such signature of charge screening effect. Therefore the Si-DB is considered to be in its neutral state for p -type doping.

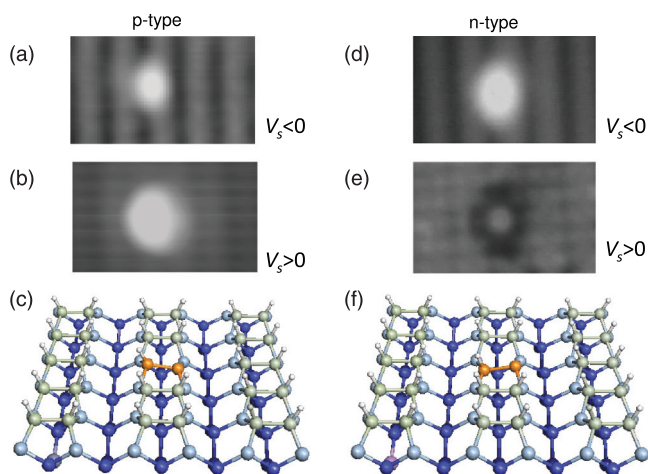


FIG. 1. (Color online) Comparison of the Si-DB structure of p - and n -type hydrogenated Si(100). (a) and (b) ($38.5 \times 22.3 \text{ \AA}^2$) occupied and unoccupied state STM topographies of a single Si-DB on the p -type doped Si(100):H surface, respectively. (c) Ball and stick sketch of the p -type Si(100):H surface. The dark blue, blue, and light blue balls are silicon atoms of the fourth, third, and second layers. The light green balls indicate the positions of the first silicon layer. The silicon dimer with the Si-DB is colored in orange. The white balls are H atoms and the grey ball is a Ga dopant atom. (d) and (e) ($38.5 \times 22.3 \text{ \AA}^2$) occupied and unoccupied state STM topographies of a single Si-DB on the n -type doped Si(100):H surface. (f) same as (c) for the n -type doped Si(100):H surface. The purple ball is an As dopant atom.

To explain why the Si-DB is in a negative charge state for n -type doped silicon whereas it is in a neutral charge state for p -type doped silicon, we calculate the electronic ground-state structure of the hydrogenated Si(100) surface and the Si-DB by using spin polarized density functional theory (DFT) and by taking into account the type of doping. The calculated spin-polarized density of states (DOS) projected onto the Si-DB and the dopant atom are shown in Figs. 2(a) and 2(b) for the p - and n -type doped silicon substrates, respectively. For p -type doping [see Fig. 2(a)], the calculated Fermi level energy is found to lie in the spin-up Si-DB state, which is therefore partly occupied. The spin-down Si-DB state is unoccupied and lies ~ 180 meV above the Fermi level. As a result, the Si-DB of the p -type doped hydrogenated Si(100) surface is close to be neutral as observed experimentally. For n -type doping [see Fig. 2(b)], the calculated Fermi level energy is found on top of the spin-up and spin-down Si-DB states. Thus two electrons occupy the Si-DB state, explaining the negative charge state of the Si-DB in this case.^{12,21,24–27} Our DFT calculations show that, from p -type to n -type doping, not only the charge state of the Si-DB is changed (from neutral to negatively charged), but the tilt angle of the silicon dimer holding the Si-DB is also modified from -9.3° (the Si-DB is in the low position) to $+7.5^\circ$ (the Si-DB is in the high position) [see Figs. 2(c) and 2(d)].

The reversible manipulation of the charge state of the Si-DB of the p -type doped hydrogenated Si(100) is performed as shown in Fig. 3. The Si-DB is first imaged with a surface voltage of $+1.7$ V as a bright feature [see Fig. 3(a)], thus indicating its neutral charge state. Then, the Si-DB is imaged at a relatively high negative surface voltage of -3.7 V. During this latter STM topography [see Fig. 3(b)], one clearly observes the hopping of the neighbor hydrogen atom from one side to the other of the silicon dimer holding the Si-DB.^{25,28} After this manipulation, the unoccupied state STM topography of the Si-DB is strongly modified as compared to the initial one [see Fig. 3(a)] and appears as a faint bright spot surrounded by a large dark halo [see Fig. 3(c)]. The similarity of this dark halo with the STM topography of the n -type doped Si-DB [see Fig. 1(e)] indicates that the Si-DB on the p -type doped hydrogenated Si(100) surface has been negatively charged upon manipulation. The probability of this negative charging process is 100% for manipulations at surface voltages between -3.7 and -2.5 V and rapidly decreases to zero for surface voltages higher than -2.5 V. The negative charge state of the Si-DB is seen to be stable for hours, even if we stop imaging with the STM for some time, move the STM tip far away from the Si-DB, and then record again the STM topography of the same area at $V_S = +1.7$ V. The manipulation of the negative charge state of the Si-DB back to its initial neutral charge state is performed as follows. The negatively charged Si-DB is imaged at a high positive surface voltage of $+3.0$ V [see Fig. 3(e)]. Afterwards, the STM topography at $V_S = +1.7$ V [see Fig. 3(f)] is identical to the initial topography of Fig. 3(a), thus indicating that the Si-DB is back in its neutral charge state. The probability of this reverse manipulation from the negative to the neutral charge state is 100% for manipulations at surface voltages higher than 2.2 V. Reversible charging and discharging have been tested over ~ 50 different Si-DBs. These results demonstrate the reversible transition

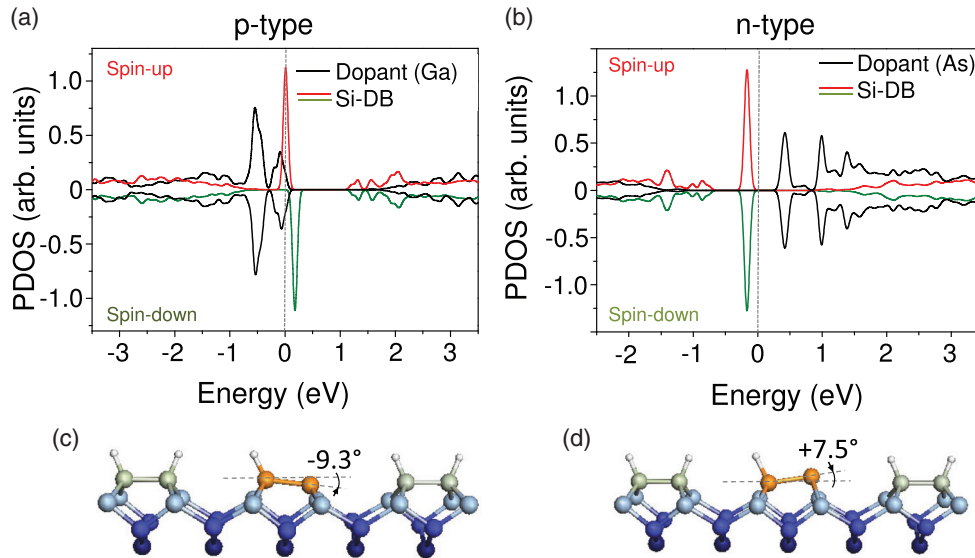


FIG. 2. (Color online) Calculation of the electronic structure of the p - and n -type doped Si(100):H surface with a Si-DB. (a) and (b) Comparison of the calculated spin polarized projected density of states (PDOS) onto the dopant atom and the Si-DB for a p - or n -type doped Si(100):H surface, respectively. (c) and (d) Ball and stick representation (side view) of the relaxed structure of the p - or n -type doped Si(100):H surface, respectively, indicating the tilt angle of the silicon dimer where the Si-DB is present.

between two stable charge states (neutral and negative) of the Si-DB.

The manipulation of the charge state of the Si-DB of the p -type doped silicon is ascribed to the electric field applied between the STM tip and the hydrogenated silicon surface. Indeed, in its initial neutral charge state, the unoccupied spin-down state of the Si-DB is located only ~ 100 meV above the Fermi level [see Figs. 2(a) and 4(a)]. Applying a negative surface voltage in the range -2.5 to -3.7 V induces downward

band bending that decreases the energy of the unoccupied spin-down state below the Fermi level [see Fig. 4(b)]. As a consequence, an electron transfer from the Si substrate to the Si-DB can be activated. To estimate the downward tip induced band bending, we solve the two-dimensional Poisson equation of the STM junction using the calculation code of Ref. 29. For

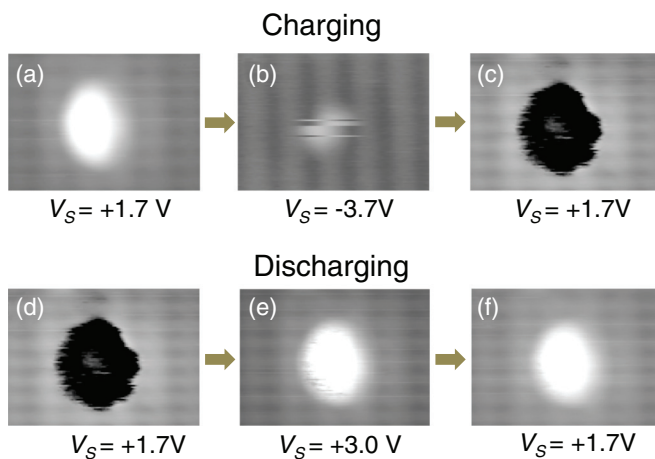


FIG. 3. (Color online) Charging and discharging of a single Si-DB on a p -type doped Si(100):H surface. (a)–(c) Series of successive ($38.5 \times 34 \text{ \AA}^2$) STM topographies recorded at various surface voltages used to induce the charging of the Si-DB. (d)–(f) Series of successive ($38.5 \times 34 \text{ \AA}^2$) STM topographies recorded at various surface voltages showing the discharging process of the Si-DB. All STM topographies are recorded on the same Si-DB with a tunnel current of 110 pA. Each STM topography takes about 40 s.

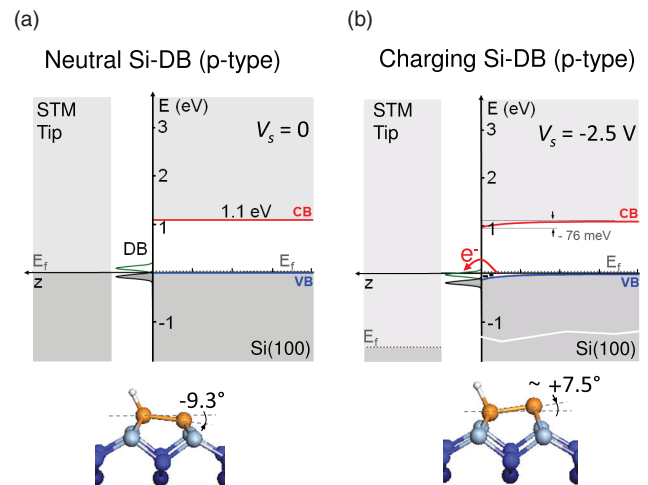


FIG. 4. (Color online) Schematic energy band diagram of the STM junction during the charging process of a single Si-DB on a p -type doped Si(100):H surface. (a) Energy band diagram of the STM junction at $V_S = 0$ V. According to the calculation of Fig. 2(a), the spin-down state energy of the Si-DB is unoccupied above the Fermi level. The Si-DB is in its neutral charge state (in average) and down position with a calculated angle of -9.3° relative to the horizontal plane. (b) Energy band diagram of the STM junction at $V_S = -2.5$ V. Due to the tip induced band bending, the two spin states of the Si-DB have energies below the Fermi level. The Si-DB is in its negative charge state and up position with an angle around $+7.5^\circ$.

a surface voltage $V_S = -2.5$ V (threshold value for negative charging), we calculate a downward band bending of -76 meV at the surface. This amount is sufficient to lower the energy of the unoccupied Si-DB state below the Fermi level [see Fig. 4(b)]. The resulting electron transfer from the silicon substrate to the Si-DB is expected to be accompanied by a change of the tilt angle of the Si dimer from -9.3° [tilt angle for the neutral charge state of the p -type doping in Fig. 4(a)] to a value close to $+7.5^\circ$ [tilt angle for the negative charge state of the n -type doping in Fig. 4(b)]. This change of the Si dimer structure is crucial to explain the stability of the negative charge state of the p -type doped Si-DB.⁸ The reverse manipulation from the negative charge state to the neutral state is therefore arising from an upward band bending when applying a positive surface voltage [see Figs. 3(d)–3(f)]. Upward band bending is shifting the negative charge state energy above the Fermi level of the Si(100) and induces electron transfer from the Si-DB to the silicon substrate. A similar gating mechanism has been proposed to explain charge localization in molecular layers on metallic surfaces.¹¹

In conclusion, we have shown that a single silicon dangling bond of a hydrogenated p -type doped Si(100) surface has two stable charge states (neutral and negative) at low temperature (5 K). Unlike previous calculations in which a Si-DB on a p -type doped Si(100):H sample is found to be positively charged at 77 K for dopant concentration ~ 0.05 Ω cm,²⁰ the trend of our work clearly indicates that a Si-DB can be initially found neutral in strongly doped Si samples (i.e., ~ 0.005 Ω cm) at 5 K. This is markedly different from the case of n -type doped Si(100) where the Si-DB has only one stable charge state (negative). It is important to note that the stabilization

of the two charge states of the p -type doped Si(100) relies on (i) the lone pair character of the Si-DB state, (ii) the proximity of the Si-DB state energies with the Fermi level, and (iii) the change of tilt angle of the silicon dimer. This demonstrates that the existence of multiple charge states of a single atom does not necessarily require the electronic decoupling between the atom and the substrate. Indeed, the Si-DB is strongly interacting, through chemical bonds, with the silicon substrate contrary to previous studies^{8–11} where the charged atom or molecule was only weakly interacting with the substrate through an insulating film and/or van der Waals interactions. Furthermore, we have shown that the charge state of the Si-DB can be reversibly changed by using a gate electric field between the STM tip and the surface. This is very similar to the operation of a flash memory³⁰ where a floating gate is reversibly charged by activating the electron transfer using a control gate. However, thousands of silicon atoms need to be charged in a single flash memory cell. Here, we have shown the reversible charge storage in a single silicon atom. This demonstrates the ultimate miniaturization of a memory cell down to a single atom, compatible with the silicon technology at 5 K. Finally, we emphasize that understanding the charging of Si-DB of p - and n -type doped hydrogen-terminated silicon is also crucial for a number of new device technologies where the use of hydrogen-terminated silicon surfaces is a key issue.³¹

This work is supported by the European Union under Project No. ICT-FET 243421 ARTIST. Calculations are performed using HPC resources from GENCI-IDRIS (Grant 2009-092042).

*Corresponding author: damien.riedel@u-psud.fr

¹Ch. Obermair, F.-Q. Xie, and Th. Schimmel, *Europhys. News* **41**(4), 25 (2010).

²M. Fuechsle, J. A. Miwa, S. Mahapatra, H. Ryu, S. Lee, O. Warschkow, L. C. L. Hollenberg, G. Klimeck, and M. Y. Simmons, *Nat. Nanotechnol.* **7**, 242 (2012).

³G. P. Lansbergen, G. C. Tettamanzi, J. Verduijn, N. Collaert, S. Biesemans, M. Blaauboer, and S. Rogge, *Nano Lett.* **10**, 455 (2010).

⁴S. Loth, M. Etzkorn, C. P. Lutz, D. M. Eigler, and A. J. Heinrich, *Science* **329**, 1628 (2010).

⁵G. P. Lansbergen, R. Rahman, C. J. Wellard, I. Woo, J. Caro, N. Collaert, S. Biesemans, G. Klimeck, L. C. L. Hollenberg, and S. Rogge, *Nat. Phys.* **4**, 656 (2008).

⁶M. Klein, J. A. Mol, J. Verduijn, G. P. Lansbergen, S. Rogge, R. D. Levine, and F. Remacle, *Appl. Phys. Lett.* **96**, 043107 (2010).

⁷K. Y. Tan, K. W. Chan, M. Möttönen, A. Morello, C. Yang, J. van Donkelaar, A. Alves, J.-M. Pirkkalainen, D. N. Jamieson, R. G. Clark, and A. S. Dzurak, *Nano Lett.* **10**, 11 (2010).

⁸J. Repp, G. Meyer, F. E. Olsson, and M. Persson, *Science* **305**, 493 (2004).

⁹F. E. Olsson, S. Paavilainen, M. Persson, J. Repp, and G. Meyer, *Phys. Rev. Lett.* **98**, 176803 (2007).

¹⁰T. Leoni, O. Guillermet, H. Walch, V. Langlais, A. Scheuermann, J. Bonvoisin, and S. Gauthier, *Phys. Rev. Lett.* **106**, 216103 (2011).

¹¹I. Fernandez-Torrente, D. Kreikemeyer-Lorenzo, A. Strozecka, K. J. Franke, and J. I. Pascual, *Phys. Rev. Lett.* **108**, 036801 (2012).

¹²M. B. Haider, J. L. Pitters, G. A. DiLabio, L. Livadaru, J. Y. Mutus, and R. A. Wolkow, *Phys. Rev. Lett.* **102**, 046805 (2009).

¹³J. L. Pitters, L. Livadaru, M. Baseer Haider, and R. A. Wolkow, *J. Chem. Phys.* **134**, 064712 (2011).

¹⁴M. Mantega, I. Rungger, B. Naydenov, J. J. Boland, and S. Sanvito, *Phys. Rev. B* **86**, 035318 (2012).

¹⁵T. C. G. Reusch, O. Warschkow, M. W. Radny, P. V. Smith, N. A. Marks, N. J. Curson, D. R. McKenzie, and M. Y. Simmons, *Surf. Sci.* **601**, 4036 (2007).

¹⁶T. H. Nguyen, G. Mahieu, M. Berthe, B. Grandidier, C. Delerue, D. Stievenard, and Ph. Ebert, *Phys. Rev. Lett.* **105**, 226404 (2010).

¹⁷M. Berthe, R. Stüflic, B. Grandidier, D. Deresmes, C. Delerue, and D. Stievenard, *Science* **319**, 436 (2008).

¹⁸P. Blaha, K. Schwarz, G. K. H. Madsen, D. Kvasnicka, and J. Luitz, *WIEN2K: An Augmented Plane Wave Plus Local Orbitals Program for Calculating Crystal Properties* (Vienna University of Technology, Vienna, Austria, 2001).

¹⁹J. P. Perdew, K. Burke, and M. Ernzerhof, *Phys. Rev. Lett.* **77**, 3865 (1996).

²⁰S. R. Schofield, P. Studer, C. F. Hirjibehedin, N. J. Curson, G. Aeppli, and D. R. Bowler, *Nat. Commun.* **4**, 1649 (2013).

- ²¹A. Bellec, D. Riedel, G. Dujardin, O. Boudrioua, L. Chaput, L. Stauffer, and P. Sonnet, *Phys. Rev. B* **80**, 245434 (2009).
- ²²G. A. Shah, M. W. Radny, Ph. V. Smith, and S. R. Schofield, *J. Phys. Chem. C*, **116**, 6615 (2012).
- ²³A. J. Mayne, D. Riedel, G. Comtet, and G. Dujardin, *Prog. Surf. Sci* **81**, 1 (2006).
- ²⁴A. Bellec, D. Riedel, G. Dujardin, N. Rompotis, and L. N. Kantorovich, *Phys. Rev. B* **78**, 165302 (2008).
- ²⁵A. Bellec, D. Riedel, G. Dujardin, O. Boudrioua, L. Chaput, L. Stauffer, and Ph. Sonnet, *Phys. Rev. Lett.* **105**, 048302 (2010).
- ²⁶L. Liu, J. Yu, and J. W. Lyding, *MRS Symposia Proceedings* (Materials Research Society, Pittsburg, 2002), Vol. 705, p. Y6.6.1.
- ²⁷S. M. Sze, *Physics of Semiconductor Devices* (Wiley-Interscience, New York, 1981).
- ²⁸K. Stokbro, U. Quaade, R. Lin, C. Thirstrup, and F. Grey, *Faraday Discuss.* **117**, 231 (2000).
- ²⁹R. M. Feenstra, *J. Vac. Sci. Technol. B* **21**, 2080 (2003).
- ³⁰Lu. Chih-Yuan, *J. Nanosci. Nanotechnol.* **12**, 7604 (2012).
- ³¹H. Yang *et al.*, *Science* **336**, 1140 (2012).